Acta Pharmacologica Sinica 2017: 1024–1037
© 2017 CPS and SIMM All rights reserved 1671-4083/17
www.nature.com/aps

Original Article

# W2476 ameliorates β-cell dysfunction and exerts therapeutic effects in mouse models of diabetes via modulation of the thioredoxin-interacting protein signaling pathway

Ting LI[1, 2, #], Guang-yao LIN[2, 3, #], Li ZHONG[1, 2, #], Yan ZHOU[1], Jia WANG[1], Yue ZHU[1,2], Yang FENG[1], Xiao-qing CAI[1], Qing LIU[1], Olivier NOSJEAN[4], Jean A BOUTIN[4], Pierre RENARD[4], De-hua YANG[1, 2], Ming-wei WANG[1, 2, 3, 5, *]

[1]*The National Center for Drug Screening and the CAS Key Laboratory of Receptor Research, Shanghai Institute of Materia Medica, Chinese Academy of Sciences, Shanghai 201203, China;* [2]*University of Chinese Academy of Sciences, Beijing 100049, China;* [3]*School of Life Science and Technology, ShanghaiTech University, Shanghai 201210, China;* [4]*Pôle d'Expertise Biotechnologie, Chimie et Biologie, Institut de Recherches SERVIER, Croissy-sur-Seine 78290, France;* [5]*School of Pharmacy, Fudan University, Shanghai 201203, China*

**Abstract**

Recent evidence shows that high glucose levels recruit carbohydrate response element-binding protein, which binds the promoter of thioredoxin-interacting protein (*txnip*), thereby regulating its expression in β-cells. Overexpression of *txnip* not only induces β-cell apoptosis but also reduces insulin production. Thus, the discovery of compounds that either inhibit TXNIP activity or suppress its expression was the focus of the present study. INS-1E cells stably transfected with either a *txnip* proximal glucose response element connected to a luciferase reporter plasmid (BG73) or full-length *txnip* promoter connected to a luciferase reporter plasmid (CL108) were used in primary and secondary high-throughput screening campaigns, respectively. From 256 000 synthetic compounds, a small molecule compound, W2476 [9-((1-(4-acetyl-phenyloxy)-ethyl)-2-)adenine], was identified as a modulator of the TXNIP-regulated signaling pathway following the screening and characterized using a battery of bioassays. The preventive and therapeutic properties of W2476 were further examined in streptozotocin-induced diabetic and diet-induced obese mice. Treatment with W2476 (1, 5, and 15 μmol/L) dose-dependently inhibited high glucose-induced TXNIP expression at the mRNA and protein levels in INS-1E cells and rat pancreatic islets. Furthermore, W2476 treatment prevented INS-1E cells from apoptosis induced by chronic exposure of high glucose and enhanced insulin production *in vitro*. Oral administration of W2476 (200 $mg \cdot kg^{-1} \cdot d^{-1}$) rescued streptozotocin-induced diabetic mice by promoting β-cell survival and enhancing insulin secretion. This therapeutic property of W2476 was further demonstrated by its ability to improve glucose homeostasis and insulin sensitivity in diet-induced obese mice. Thus, chemical intervention of the TXNIP-regulated signaling pathway might present a viable approach to manage diabetes.

**Keywords:** diabetes; glucose; TXNIP; β-cells; W2476; high-throughput screening

*Acta Pharmacologica Sinica* (2017) 38: 1024–1037; doi: 10.1038/aps.2017.15; published online 15 May 2017

## Introduction

Thioredoxin-interacting protein (TXNIP), also known as vitamin $D_3$ up-regulated protein 1 (VDUP1)[1] or thioredoxin-binding protein-2 (TBP-2)[2], is a ubiquitously expressed protein with a molecular weight of 50 kDa. It was initially identified as a negative regulator of thioredoxin[2–4] to mediate cellular oxidative stress[3–7]. Subsequent investigations have demonstrated that TXNIP regulates a wide variety of physiological processes, including cell growth, differentiation and death, energy metabolism and immune responses[8–11].

A recent study showed that high concentrations of glucose could substantially increase the mRNA and protein levels of TXNIP in multiple β-cell lines and cultured islets of Langerhans from different mouse models of type 1 or type 2 diabetes[12–14]. One of the underlying mechanisms is that glucose recruits carbohydrate response element-binding protein (ChREBP), which binds the carbohydrate response element (ChoRE) located in the promoter of *txnip*[13–15]. Given that

# These authors contributed equally to this work.
*To whom correspondence should be addressed.
E-mail: mwwang@simm.ac.cn
Received 2016-12-26 Accepted 2017-02-09

persistent hyperglycemia is a common manifestation of type 2 diabetes mellitus (T2DM) and its expression is rapidly and vigorously induced by glucose, TXNIP was proposed to be a key link between hyperglycemia and β-cell dysfunction[13, 16, 17], insulin production[18] and insulin resistance[19].

It is known that TXNIP can induce cell apoptosis in response to oxidative stress[20]. β cells have low levels of antioxidant enzymes[21] and thus are more susceptible to apoptosis upon TXNIP overexpression[17]. TXNIP deficiency in the pancreas increases β-cell mass by inhibition of apoptosis[16, 22, 23]. TXNIP has been found to decrease insulin transcription by directly targeting or indirectly down-regulating v-maf musculoaponeurotic fibrosarcoma oncogene family protein A (MafA), a known insulin transcription factor[18]. TXNIP was also implicated in modulating insulin sensitivity by disrupting insulin-stimulated glucose uptake in the skeletal muscle and adipocytes[23–25]. Several studies using HcB-19 (*txnip* nonsense mutation), β-cell-specific *txnip* knockout (βTKO) and *txnip* deleted *ob/ob* mice supported the proposition that the inhibition of TXNIP is potentially a novel approach to combat type 1 and type 2 diabetes[10, 16, 23, 26, 27] by promoting β-cell survival and improving insulin sensitivity.

To date, no small molecule that can effectively modulate glucose-induced TXNIP overexpression has been reported. Here, we describe a high-throughput screening (HTS) assay that was applied to discover such modulators leading to the identification of W2476, a synthetic compound capable of lowering TXNIP expression induced by high concentrations of glucose. Therefore, the present study was designed to investigate the bioactivities of W2476 in β-cells both *in vitro* and *in vivo*.

## Materials and methods

### Chemistry

#### *General statement*

Reagents were of commercial grade and used as received unless otherwise noted. All new compounds were judged to be ≥95% pure by HPLC. NMR spectra were recorded on Varian Mercury 300 (Varian, Palo Alto, CA, USA). Chemical shifts were reported in parts per million (ppm), with the solvent resonance as the internal standard ($CDCl_3$ 7.27 ppm for $^1$H NMR, 77.23 ppm for $^{13}$C NMR, DMSO-$d_6$ 2.50 ppm for $^1$H NMR, 39.51 ppm for $^{13}$C NMR). Low-resolution mass spectral data (electrospray ionization) were acquired on a Finnigan LCQ-DECA mass spectrometer (Thermo Finnigan, Altrincham, Cheshire, UK). High-resolution mass spectral data (TOF) were acquired on an Agilent 6224 mass spectrometer (Agilent, Santa Clara, CA, USA). Samples were analyzed for purity on an HP1100 series (Agilent) equipped with a Zorbax SB-C18 column (5 μm, 4.6 mm×250 mm). Purities of final compounds were determined using a 5-μL injection with quantification by AUC at 210 nm and 254 nm (Agilent diode array detector).

#### *1-(4-(2-Bromoethoxy)phenyl)ethanone*

4′-Hydroxyacetophenone ($M_w$ = 136.1, 5 g, 0.0367 mol, 1 eq) was added to the mixture of 1,2-dibromoethane ($M_w$ = 187.9, d=2.17 g/mL, 24.05 mL, 0.2778 mol, 7.57 eq), potassium carbonate ($M_w$=138.2, 17.87 g, 0.129 mol, 3.5 eq) and triethylbenzylammonium chloride (TEBA, catalytic amount) in ethyl acetate (100 mL) at 60 °C. The reaction was refluxed overnight. After cooling, water was added and the mixture was extracted with ethyl acetate (3×50 mL). The organic phase was washed with 1 mol/L NaOH solution and water, and then dried over anhydrous sodium sulfate. After filtration, the solvent was removed *in vacuo,* and the residue was separated on the Biotage SNAP cartridge KP-Sil 340 g column (Biotage, Shanghai, China) eluting with 30% ethyl acetate/petroleum ether. The product was obtained as yellowish oil, which was solidified after cooling (7.99 g, yield: 89.6%). The purity was 97.0% by HPLC analysis. LR-ESI: 264.0 $(M+Na)^+$. HR-MS (TOF) $m/z$ calcd for $C_{10}H_{12}BrO_2$ $[M+H]^+$ 243.0021, found 243.0023. $^1$H NMR ($CDCl_3$, 300 MHz) $\delta$ 2.57 (s, 3H), 3.67 (t, $J$ = 6.3 Hz, 2H), 4.36 (t, $J$ = 6.3 Hz, 2H), 6.95 (d, $J$ = 8.4 Hz, 2H), 7.95 (d, $J$ = 8.7 Hz, 2H). $^{13}$C NMR ($CDCl_3$, 75 MHz) $\delta$ 26.5, 29.8, 68.0, 114.4 (3C), 130.8 (2C), 162.0, 196.8.

#### *9-((1-(4-Acetylphenyloxy)ethyl)-2-)adenine*

Potassium carbonate ($M_w$ = 138.2, 0.27 g, 1.98 mmol, 2 eq) was added into the mixture of adenine ($M_w$ = 135.1, 0.13 g, 0.99 mmol, 1 eq) and 1-(4-(2-bromoethoxy)phenyl)ethanone ($M_w$=243.1, 0.30 g, 1.23 mmol, 1.25 eq) in anhydrous DMF (30 mL). Then, the reaction was stirred at 80 °C overnight. After cooling, it was filtered and the solution was evaporated *in vacuo* to obtain the crude product, which was further recrystallized with ethanol to obtain the pure product (0.23 g, yield: 79.3%).The purity was 96.0% by HPLC analysis. LR-ESI: 319.2 $(M+Na)^+$. HR-MS (TOF) $m/z$ calcd for $C_{15}H_{16}N_5O_2$ $[M+H]^+$ 298.1304, found 298.1309. $^1$H NMR (DMSO-$d_6$, 300 MHz) $\delta$ 2.50 (s, 3H), 4.47 (t, $J$ = 5.1 Hz, 2H), 4.57 (t, $J$ = 4.8 Hz, 2H), 7.03 (d, $J$ = 8.4 Hz, 2H), 7.20 (brs, 2H, $NH_2$), 7.90 (d, $J$ = 8.4 Hz, 2H), 8.16 (s, 1H), 8.19 (s, 1H). $^{13}$C NMR (DMSO-$d_6$, 75 MHz) $\delta$ 26.4, 42.4, 66.0, 114.4 (2C), 118.6, 130.3, 130.5 (2C), 141.2, 149.6, 152.5, 156.0, 161.8, 196.3.

### Reagents

Antibodies against TXNIP (JY2), MafA (F-6) and ChREBP and those used in Western blotting were purchased from MBL International (Woburn, MA), Santa Cruz Biotechnology (Santa Cruz, CA, USA) and Cell Signaling Technology (Danvers, MA, USA), respectively.

### Cell culture

L6 myoblasts were cultured in DMEM containing 10% FBS. Upon differentiation, the concentration was decreased to 2%. Culture and differentiation of 3T3-L1 cells were conducted according to the literature[28]. Islets of Langerhans from Sprague-Dawley rats and mice were prepared using a collagenase digestion procedure as described previously[29]. Mouse hepatocytes were isolated using Selgen's two-step perfusion method[30]. INS-1E cells and islets were cultured in RPMI-1640, and hepatocytes were maintained in DMEM. INS-1E cells were stably transfected with either a human *txnip*

proximal glucose response element connected to a luciferase reporter plasmid (BG73) or a full-length human *txnip* promoter connected to a luciferase reporter plasmid (CL108) and maintained in RPMI-1640 in the presence of 50 μg/mL geneticin (Life Technologies, Carlsbad, CA, USA). Information about the TXNIP construct promoter sequences is available upon request.

#### RNA extraction and quantitative real-time PCR

Total RNA from INS-1E cells, L6 myoblasts, 3T3-L1 cells, hepatocytes and rat islets were extracted using TRIzol reagent (Life Technologies) according to the manufacturer's instructions. RNA was converted to cDNA using a High-Capacity cDNA Reverse Transcription kit (Life Technologies), and quantitative real-time PCR was performed using SYBR Green Master Mix (DRR820A; Takara, Dalian, China) on an ABI ViiA7 system (Life Technologies). The primers used are shown in Table S1. All the samples were analyzed in triplicate, and *gapdh* was used as an internal control.

#### Annexin V-FITC/PI double-labeled flow cytometry

INS-1E cells were cultured in RPMI-1640 (2 % FBS) in the presence of 5 mmol/L or 33.3 mmol/L glucose with or without different concentrations of W2476 for 48 h. Apoptotic cells were identified using the Dead Cell Apoptosis Kit with Annexin V-FITC and PI (Life Technologies) according to the manufacturer's instructions. Flow cytometry data were acquired using an Accuri C6 Flow Cytometer (BD Biosciences, San Jose, CA, USA) and analyzed using Accuri C6 software.

#### Western blot analysis

Protein extracts from W2476-treated INS-1E cells were prepared according to the procedure published previously[17]. The following antibodies were used: TXNIP (1:400), MafA (F-6) (1:500), insulin (1:1000), cleaved caspase-3 (1:500), caspase-3 (1:1000), cleaved caspase-9 (1:1000), caspase-9 (1:1000), ChREBP (1:200), β-actin (1:2000), GAPDH (1:2000), goat anti-mouse IgG (1:8000) and goat anti-rabbit IgG (1:8000). Signals were detected by a ChemiDoc™ MP Imaging System from Bio-Rad Laboratories (Richmond, CA, USA).

#### Animal studies

All animal experimentation was conducted in accordance with the regulations adopted by the Animal Care and Use Committee, Shanghai Institute of Materia Medica, Chinese Academy of Sciences (approval number: 2014-SIMM-06).

A detailed flowchart of animal study procedures was shown in Figure S1. Briefly, male C57BL/6 mice (SLAC Laboratory Animal Co, Ltd, Shanghai, China) were kept in a temperature-controlled room (22±2 °C), with a light/dark cycle of 12 h. Mice of 8 weeks of age were injected with streptozotocin (STZ; 40 $mg \cdot kg^{-1} \cdot d^{-1}$ for 5 d, freshly prepared in 0.1 mmol/L sodium citrate; pH 4.3–4.5) according to the procedure published previously[31]. For studying the preventive or therapeutic effect of W2476 on STZ-induced diabetic mice, either vehicle (0.5% methylcellulose, MC) or W2476 (200 $mg \cdot kg^{-1} \cdot d^{-1}$) was orally administered, respectively. Verapamil (positive control; Sigma, St Louis, MO, USA) was given in the drinking water (1 mg/mL, equivalent to an average dose of 100 $mg \cdot kg^{-1} \cdot d^{-1}$). Body weight and food intake were monitored daily, and blood glucose levels from 6-h fasting mice were measured. For the oral glucose tolerance test (OGTT), a bolus of 2 g/kg glucose was delivered to 6-h fasting mice, and blood glucose levels were determined at designated time points. At the end of the study, plasma insulin level was assessed using a mouse insulin ELISA kit (EZRMI-13K; Millipore, Temecula, CA, USA). The pancreas was removed from euthanized mice and subsequently fixed in 4% paraformaldehyde (PFA) for immunohistochemistry or for isolating the islets.

Four-week-old male C57BL/6J mice were fed on a high-fat diet (HFD; D12492, Research Diet, New Brunswick, NJ, USA) to establish a diet-induced obese (DIO) model or a standard chow diet (SCD; D12450B, Research Diet) and watered *ad libitum*. After 4- or 12-week HFD feeding, they were randomly assigned to 4 treatment groups ($n$=9–12 per group) with matched body weight: (1) 0.5% *w/v* methylcellulose (MC), (2) 200 $mg \cdot kg^{-1} \cdot d^{-1}$ oral W2476, (3) 400 $mg \cdot kg^{-1} \cdot d^{-1}$ oral W2476, and (4) 100 $mg \cdot kg^{-1} \cdot d^{-1}$ verapamil contained in drinking water (1 mg/mL). Body weight and food intake were recorded daily, and 6-h fasting blood glucose levels were measured every three weeks. Following a 4-h fasting period, an insulin tolerance test (ITT) was performed by intraperitoneal injection of 2.5 IU/kg insulin to measure blood glucose levels thereafter. At the end of 6-week treatment, samples were collected to examine insulin levels and the expression of TXNIP. Plasma biochemical indices were analyzed as described previously[32].

#### Immunohistochemistry

Immunofluorescence imaging analysis was carried out as previously described[32]. Briefly, the pancreas was fixed with 4% PFA, embedded in paraffin, and sliced into 4-μm cross sections. Insulin and glucagon were stained with anti-insulin (1:200) or anti-glucagon (1:200; Abcam, Cambridge, MA, USA) antibodies, respectively. The nuclei were visualized with 4′,6-diamidino-2-phenylidole (DAPI).

#### Statistical analysis

Data are presented as means±SEM and analyzed by Student's *t*-test or one-way ANOVA. $P<0.05$ was considered to be statistically significant.

## Results

#### HTS assay development and compound screening

Expression of the luciferase reporter gene can be stimulated by various concentrations of glucose in both BG73 and CL108 cells, with $EC_{50}$ values of 9.74±0.42 mmol/L and 9.48±0.95 mmol/L, respectively. BG73 cells responded to glucose stimulation more sensitively than did CL108 cells, with a greater response window of 7.36 times at 25 mmol/L glucose. The reporter gene in BG73 cells was fully activated at glucose concentrations equal to or above 16.7 mmol/L (Figure S2A). Thus, 19.4 mmol/L glucose was used in the HTS campaigns

with BG73 cells. The BG73 assay system showed coefficient of variation (CV) values of 5.94% for high glucose (HG, 19.4 mmol/L) and 7.12% for basal glucose (BG, 3.3 mmol/L), a signal-to-background ratio of 6.91 and a Z′ factor of 0.72 (Figure S2B). These parameters indicate that the assay system was of high quality and well suited to HTS[33]. Of the 256 000 synthetic compounds from the collection of the Chinese National Compound Library screened, 892 (0.34%) initial hits were identified using 80% inhibition as the cut-off line (Figures S1C, S1D). They subsequently went through a secondary screening involving both BG73 and CL108 cells that yielded 4 confirmed hits (0.45% or an overall hit rate of 0.02‰).

### W2476 modulates TXNIP expression in INS-1E cells

Following the above confirmation studies, we selected one compound, WNN2476-A011 [W2476, 9-((1-(4-acetylphenyloxy)-ethyl)-2-)adenine, Figure 1A and Figure S3], as a model for further characterization. W2476 concentration-dependently suppressed reporter gene expression in BG73 cells with $IC_{50}$ values of 1.7±0.1 μmol/L at HG (19.4 mmol/L) or 3.1±0.6 μmol/L at BG (3.3 mmol/L), respectively (Figures 1B). In CL108 cells, the $IC_{50}$ of W2476 was 3.3±0.6 mmol/L at HG, with no concentration-dependent response at BG (Figure 1C), implying that it did not inhibit TXNIP expression at BG, which might allow TXNIP to retain other functions[34–38].

To investigate whether W2476 could affect TXNIP expression in INS-1E cells, we treated the cells with 5 mmol/L or 25 mmol/L glucose for 6, 12, 24 and 48 h in the presence or absence of W2476 (10 μmol/L). Western blot analysis illustrated that 25 mmol/L glucose could significantly increase TXNIP expression from 6 h to 48 h, which was completely inhibited by 10 μmol/L W2476 (Figure 1D). W2476 at 1, 5 and

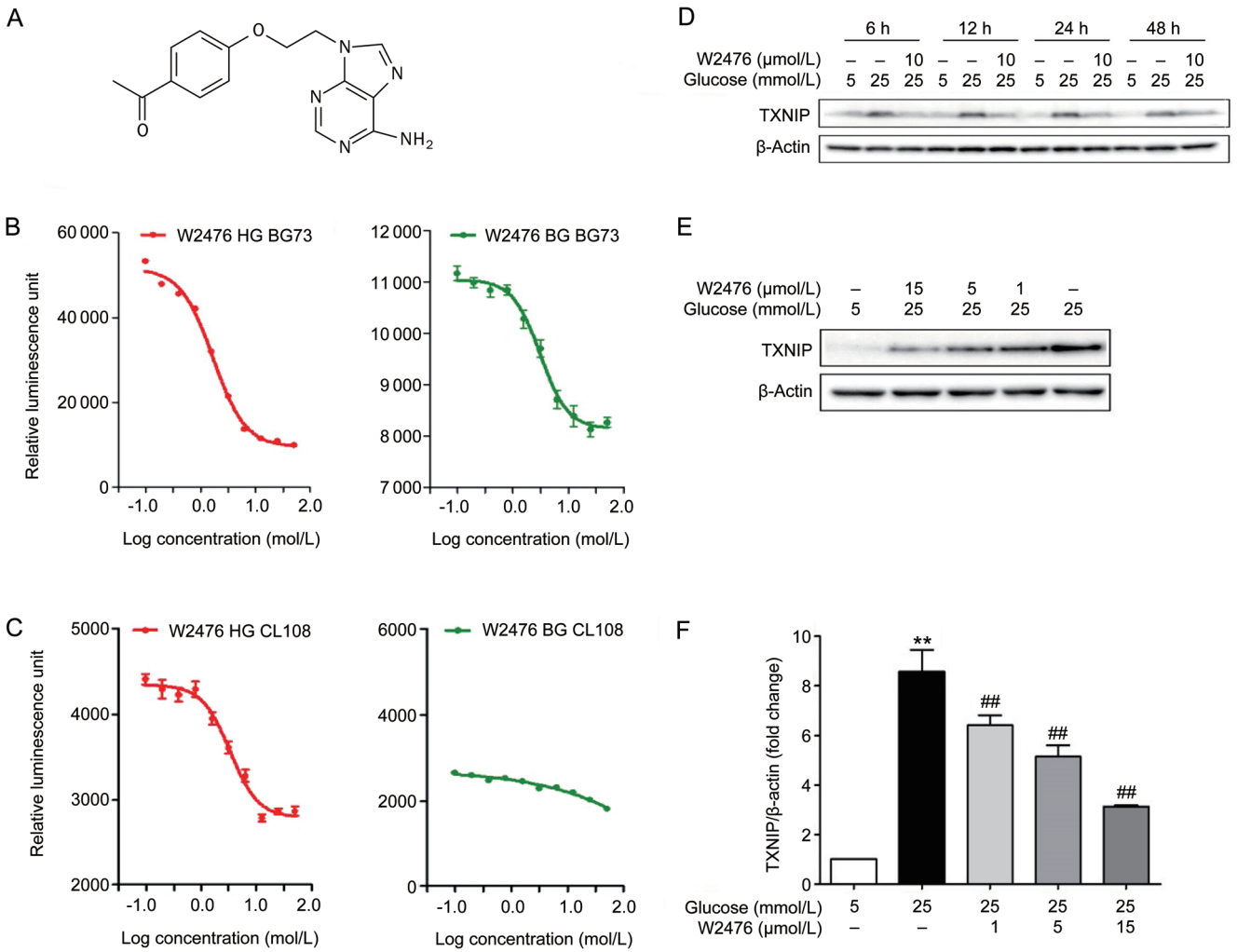


**Figure 1.** Structure of W2476 and its characterization in BG73, CL108 and INS-1E cells. (A) Chemical structure of W2476 ($C_{15}H_{15}N_5O_2$, $M_w$: 297.31). BG73 or CL108 used for counter screening were treated with either 19.4 mmol/L or 3.3 mmol/L glucose with or without different concentrations of W2476 for 24 h. The reporter gene activity was evaluated and the modulating activity of W2476 was examined under high glucose (HG, 19.4 mmol/L) and basal glucose (BG, 3.3 mmol/L) conditions in both BG73 (B) and CL108 (C) cells. INS-1E cells were treated with 10 μmol/L W2476 in the presence of 5 mmol/L or 25 mmol/L glucose for 6, 12, 24 or 48 h (D), or with different doses of W2476 for 24 h (E, F), followed by immunoblotting of TXNIP. Values represent means±SEM for three independent experiments. $^{**}P<0.01$ *vs* 5 mmol/L glucose. $^{\#\#}P<0.01$ *vs* 25 mmol/L glucose.

15 μmol/L suppressed TXNIP expression by 25.31% ($P$<0.01), 40.09% ($P$<0.01) and 63.54% ($P$<0.001; Figures 1E, 1F), respectively. These data demonstrate that the modulating effect of W2476 on TXNIP was both time- and concentration-dependent. The repressive property of W2476 on TXNIP expression was also observed in mouse hepatocytes, L6 myotubes and 3T3-L1 adipocytes (Figure S4).

#### W2476 inhibits high glucose-induced apoptosis

INS-1E cells were treated with 5 mmol/L or 33.3 mmol/L glucose for 48 h and subjected to various concentrations of W2476, followed by detection of TXNIP expression and cell apoptosis. We found that W2476 could significantly decrease TXNIP expression at 33.3 mmol/L glucose (Figures 2A, 2B). Cell apoptosis was evaluated, revealing that 33.3 mmol/L glucose induced INS-1E cell apoptosis, which could be rescued by 10 μmol/L and 15 μmol/L W2476 (Figures 2C, 2D).

We also examined activation of caspases, critical biomarkers of cell apoptosis, in INS-1E cells. Western blot analysis showed that 33.3 mmol/L glucose increased the cleavage of caspase-3, which could be dose-dependently inhibited by W2476 (Figures 2E–2G). Moreover, W2476 exerted similar effects on the cleavage of caspase-9 (Figures 2H–2J). These results indicate that W2476 was able to reverse high glucose-induced INS-1E cell apoptosis.

#### W2476 elevates insulin and MafA expression

Because TXNIP has been proposed to down-regulate the transcription of *mafA* and *insulin*, we investigated whether W2476 could reverse the impact of high glucose on MafA and insulin via reduction of TXNIP expression. INS-1E cells were incubated for 24 h with 5 mmol/L or 25 mmol/L glucose in the presence or absence of W2476, followed by analysis of gene and protein expression. In comparison to 5 mmol/L, 25 mmol/L glucose significantly attenuated insulin expression at both the mRNA and protein levels, which were accompanied by an increase in TXNIP expression. As TXNIP was diminished by W2476, MafA and insulin gene (Figures 3A–3C) and protein (Figures 3D–3F) expression were increased in a concentration-dependent manner. Isolated rat islets of Langerhans were also applied to verify this effect of W2476, in which islets were exposed to 33.3 mmol/L glucose with or without 15 μmol/L W2476 for 48 h. It was shown that W2476 decreased TXNIP mRNA level by 2-fold, and this reduction was accompanied by an increase in *insulin* transcription (Figures 3G–3H). However, changes in *mafA* transcription were not observed under this condition (Figure 3I).

#### Therapeutic property of W2476 in STZ-induced diabetic mice

Previous studies suggest that genetic deletion and pharmacological inhibition of TXNIP were able to protect animals against STZ-induced diabetes[16, 39, 40]. In this study, STZ-induced diabetic mice were employed to examine whether W2476 exerts a similar effect via modulating TXNIP. After treatment with W2476 or verapamil for 3 d, mice were intraperitoneally (ip) injected with STZ (40 $mg \cdot kg^{-1} \cdot d^{-1}$) for 5 d (d 4 to 8). As shown in Figure 4A, while 6-h fasting blood glucose in the control group reached 10.64±0.88 mmol/L (diabetic state) on d 17, that of verapamil- or W2476-treated mice remained normal (7.77±0.41 mmol/L and 7.78±0.38 mmol/L, respectively). This phenomenon was accompanied by a 49% and 37% reduction of TXNIP protein levels in W2476- and verapamil-treated group, respectively (Figures 4B, 4C). To evaluate islet function, OGTT was performed, and 15.04% and 20.77% reduction of the area under the curve ($AUC_{0-120}$) for blood glucose levels were found in mice treated with either 100 mg/kg verapamil or 200 mg/kg W2476 compared to vehicle-treated control ($P$<0.05 and $P$<0.01, respectively; Figures 4D, 4E). In addition, immunohistochemistry revealed that islet structure was severely disrupted, with poor insulin staining in STZ-treated mice, whereas normal insulin-containing islets were observed in both verapamil- and W2476-treated groups (Figure 4F).

To further investigate whether W2476 could reverse overtly STZ-induced diabetes, C57BL/6 mice were given daily STZ (40 $mg \cdot kg^{-1} \cdot d^{-1}$) ip injection for 5 d and rested for 10 d. Staring from d 15, mice divided into three groups were treated with W2476 (200 $mg \cdot kg^{-1} \cdot d^{-1}$), verapamil (100 $mg \cdot kg^{-1} \cdot d^{-1}$) or vehicle (0.5% MC) for the next 10 d. As depicted in Figure 5A, fasting blood glucose levels in verapamil- and W2476-treated groups were both reduced by 27.7% on d 25. The OGTT study showed that glucose $AUC_{0-120}$ values in W2476- and verapamil-treated animals were reduced by 23.8% and 21.8%, respectively ($P$<0.01 and $P$<0.01; Figures 5B, 5C). This was accompanied by parallel increases in plasma insulin levels by 34.43% (W2476) and 34.65% (verapamil) compared to STZ control (Figure 5D). Immunofluorescence staining of pancreatic cross-sections exhibited severe islet destruction in the STZ group, whereas normal morphology and intensive insulin staining were observed in W2476- and verapamil-treated animals (Figure 5E).

#### Preventive and therapeutic properties of W2476 in DIO mice

To study whether chronic administration of W2476 exerts protective or therapeutic effect in DIO mice, we fed C57BL/6 mice with HFD either for 4 weeks to create a pre-obese state, or for 12 weeks to present overweight, hyperglycemic, hyperinsulinemic and dyslipidemic features[41]. This was followed by 6-week daily treatment of either W2476 (200 mg/kg or 400 mg/kg) or verapamil (100 mg/kg). While the body weight on the last day of dosing and the average food intake during the 6-week treatment period did not significantly alter between HFD control and treatment groups in both preventive (Figures 6A, 6B) and therapeutic experiments (Figures 7A, 7B), significant reduction in fasting blood glucose and plasma insulin levels were observed after the treatment (Figures 6C, 6F, 7C, 7D). This was accompanied by improved ITT responses in W2476- but not verapamil-treated mice (Figures 6G, 6H, 7E, 7F). To determine if the above beneficial effects are mediated via inhibition of TXNIP and the difference between W2476 and verapamil, we examined the level of TXNIP in metabolism-related organs after treatment. W2476, but not verapamil,

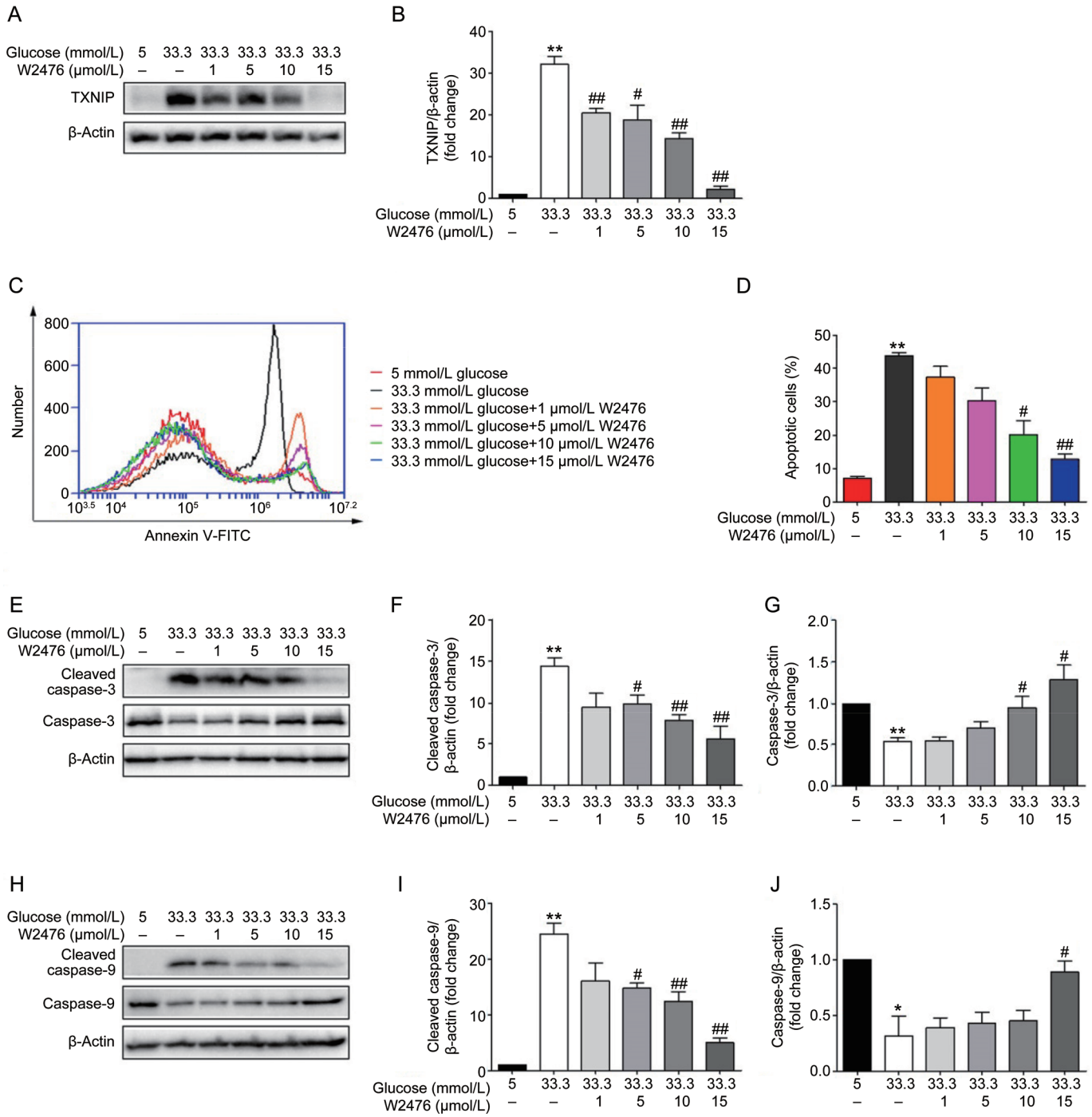


**Figure 2.** Effect of W2476 on high glucose-induced INS-1E cell apoptosis. INS-1E cells were incubated at 5 mmol/L or 33.3 mmol/L glucose in the presence or absence of varying concentrations of W2476 with 2% FBS for 48 h. (A, B) Protein expression levels of TXNIP were measured by Western blotting. (C, D) Cell apoptosis was assessed by flow cytometry using Annexin V/PI staining. Immunoblotting of cleaved caspase-3 (E, F) and caspase-3 (E, G) as well as cleaved caspase-9 (H, I) and caspase-9 (H, J) after treatment with W2476. Representative immunoblots were shown and protein contents were separately quantified. All values are presented as mean±SEM of at least three independent experiments; $^{*}P<0.05$, $^{**}P<0.01$ *vs* 5 mmol/L glucose; $^{\#}P<0.05$, $^{\#\#}P<0.01$ *vs* 33.3 mmol/L glucose.

significantly decreased pancreatic TXNIP expression (Figures 6D, 6E). Neither W2476 nor verapamil exhibited any inhibitory effect on TXNIP in the subcutaneous fat, liver and skeletal muscle (Figure S5). Pharmacokinetic analysis suggests that this differentiated action of W2476 may have resulted from its different tissue distribution (Figure S6, Tables S2, S3).

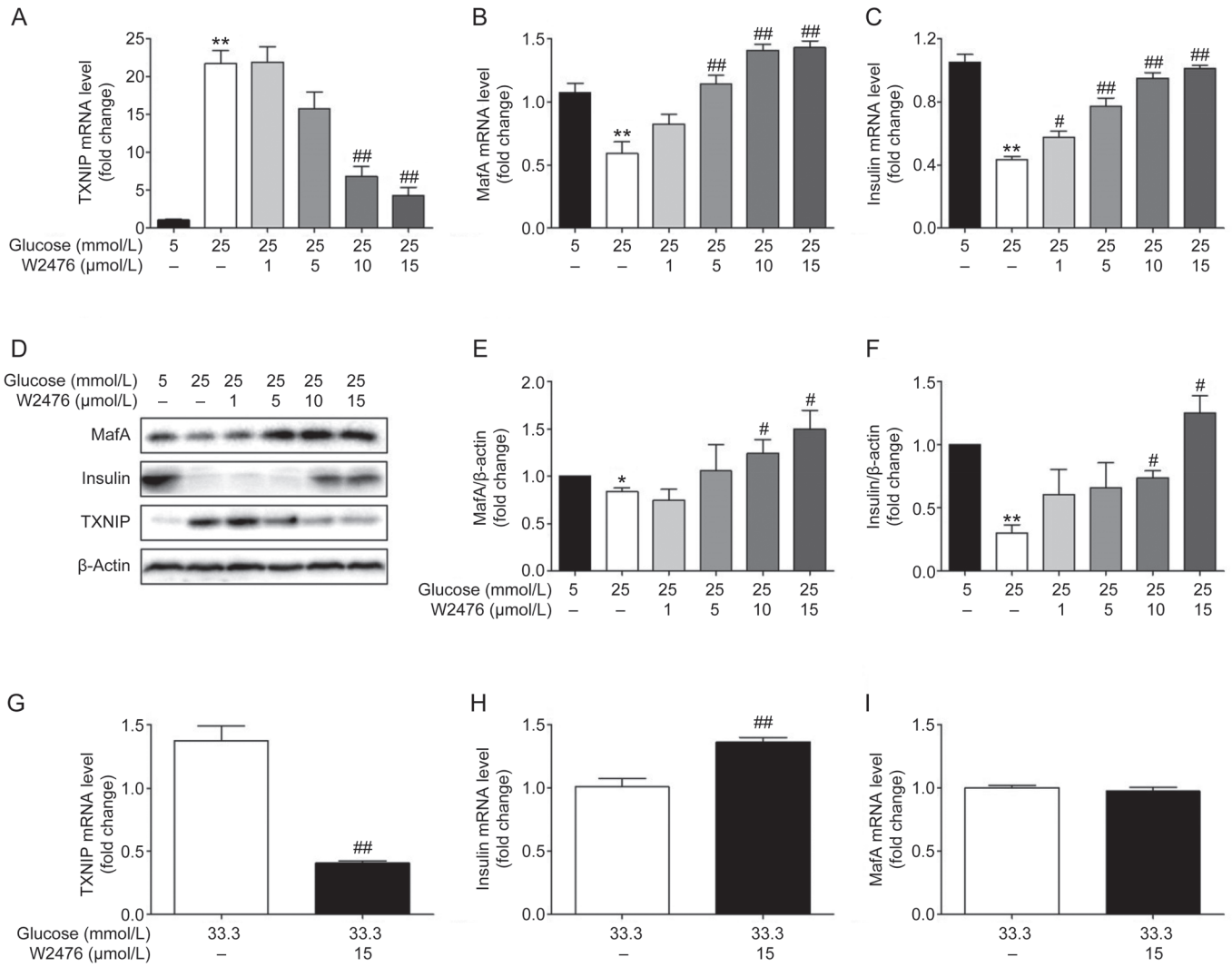


**Figure 3.** Effects of W2476 on insulin and MafA expression. INS-1E cells were exposed to 5 mmol/L or 25 mmol/L glucose with or without varying concentrations of W2476 for 24 h, followed by measurement of mRNA levels of *txnip* (A), *mafa* (B) and *insulin* (C) using quantitative real-time PCR. Protein levels of TXNIP (D), MafA (D, E) and insulin (D, F) were evaluated by Western blotting. Representative immunoblots were shown and protein contents were separately quantified. Isolated rat islets of Langerhans were incubated for 48 h with 33.3 mmol/L glucose and 15 μmol/L W2476, and mRNA levels of *txnip* (G), *insulin* (H) and *mafa* (I) were assessed by quantitative real-time PCR. Data shown are mean±SEM of three independent experiments. $^{*}P<0.05$, $^{**}P<0.01$ *vs* 5 mmol/L glucose. $^{\#}P<0.05$, $^{\#\#}P<0.01$ *vs* 25 mmol/L glucose in A–F. $^{\#\#}P<0.01$ *vs* 33.3 mmol/L glucose in G–H.

At the end of the 6-week therapy, the plasma triacylglycerol level was markedly elevated in the HFD control, which was significantly reversed by W2476; no significant difference was found in plasma cholesterol and nonesterified fatty acid levels among the treatment groups in two experimental settings (Tables S4, S5). We also compared the low-density lipoprotein-cholesterol/high-density lipoprotein-cholesterol (LDL-C/HDL-C) ratio in these animals, showing that long-term exposure to HFD increased the LDL/HDL ratio by 61.5%, which was decreased by 9.52% (200 mg/kg, $P<0.05$) and 23.81% (400 mg/kg, $P<0.01$) after two doses of W2476 administration (Table S5). This phenomenon was not observed in mice that received prophylactic W2476 treatment (Table S4).

## Discussion

ChREBP shuttling from the cytoplasm to nucleus binds to the ChoRE in the promoters of many genes[42] involved in glycolysis, lipogenesis and gluconeogenesis[42, 43]. Among them, TXNIP shows prominence[15]. Therefore, a search for small molecules capable of modulating ChREBP and the downstream signaling pathway is of interest.

ChREBP mainly regulates the expression of TXNIP in pancreatic β-cells. The link between TXNIP and diabetes has been recently strengthened with identification of effective modulators of TXNIP. Exenatide, a marketed anti-diabetic drug, was shown to suppress TXNIP expression in INS-1E cells and primary islets, leading to increased β-cell mass[22]. Verapamil,

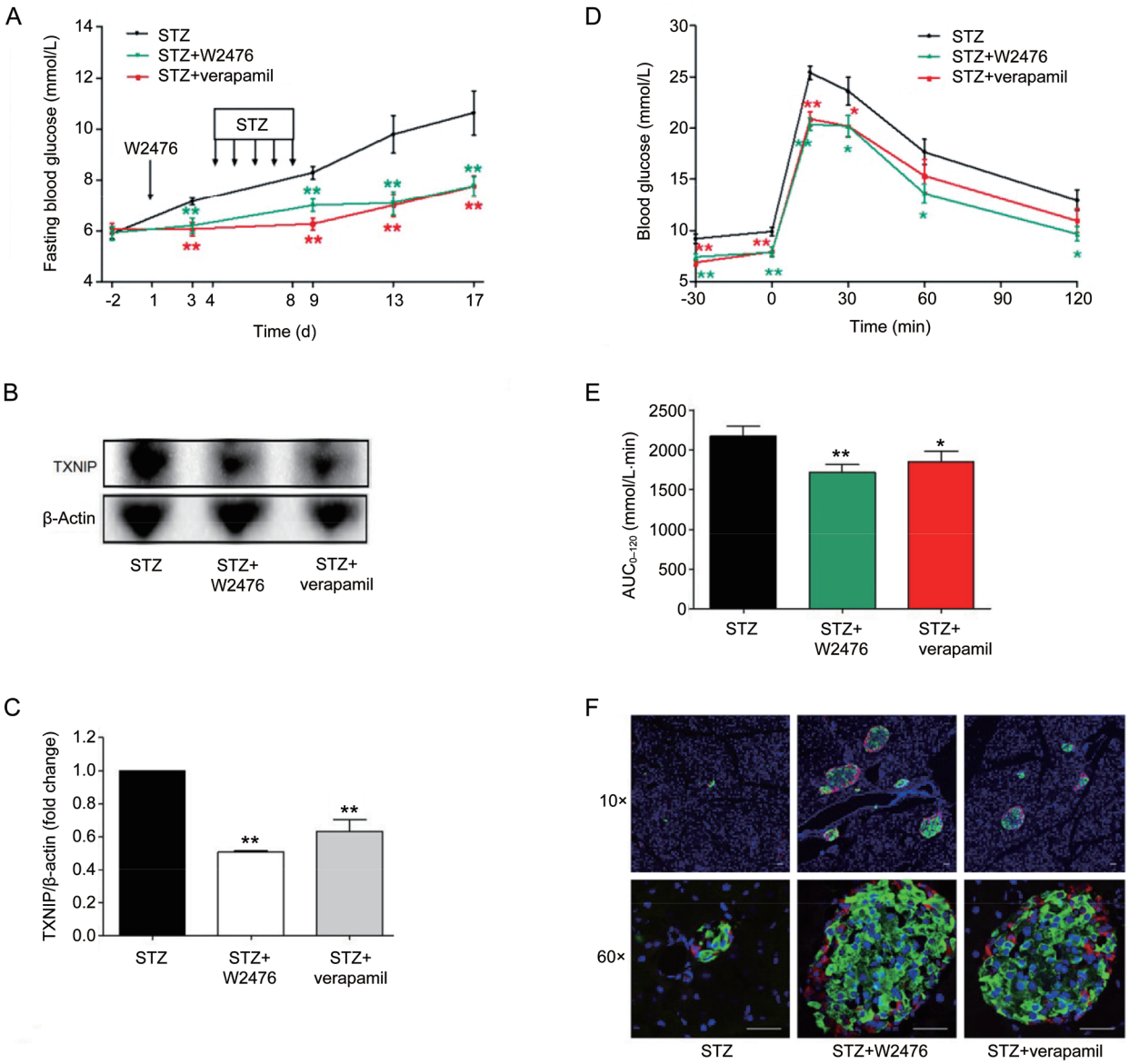


**Figure 4.** Protective effect of W2476 on STZ-induced diabetic mice. Male C57BL/6 mice received either verapamil in drinking water (100 mg·kg$^{-1}$·d$^{-1}$) or an oral dose of W2476 (200 mg·kg$^{-1}$·d$^{-1}$) between d 1 and 17. Three days after the treatment, all groups received daily intraperitoneal injection of STZ (40 mg·kg$^{-1}$·d$^{-1}$) for 5 d. (A) Blood glucose levels at indicated times minus baseline values measured on d 3 ($n$=12 per group). (B, C) Effects of W2476 and verapamil on pancreatic islet TXNIP protein levels in each group. On d 17, OGTT was performed to assess blood glucose levels (D) and the glucose area-under-the-curve integrated from 0 to 120 min ($AUC_{0-120}$; E) in all treatment groups. (F) Immunofluorescence staining of pancreatic islets prepared from three groups after 17-d treatment. Red, glucagon; green, insulin; blue, nuclei/DAPI. Scale bar, 30 μm. Original magnification, 10× (upper panel) and 60× (lower panel). Data shown are mean±SEM. $^{*}P$<0.05, $^{**}P$<0.01 *vs* STZ group.

a calcium channel blocker, was also found to inhibit TXNIP expression in β-cells and exert a therapeutic effect on several diabetic animal models. However, the concentration of verapamil that inhibited TXNIP was extremely high (50 mmol/L) *in vitro,* suggesting its poor efficacy[31]. In this paper, we present a small molecule, W2476, as a modulator of TXNIP expression discovered by HTS and characterized using a battery of *in vitro* and *in vivo* bioassays.

A human microarray study initially established that TXNIP was powerfully stimulated by glucose[44] and may play an important role in the pathogenesis of T2DM[45]. It is known that transcription of *txnip* is regulated by glucose, and its promoter has a ChoRE site crucial for glucose-induced ChREBP/Mlx heterodimer binding in β-cells[15]. BG73 cells with proximal elements of ChoRE in the *txnip* promoter were more sensitive to glucose in our reporter assay used for primary screening. Because CL108 cells with an intact *txnip* promoter responded to glucose in a manner similar to induction of TXNIP expression under physiological conditions, they were applied to secondary screening. Of note, W2476, identified by

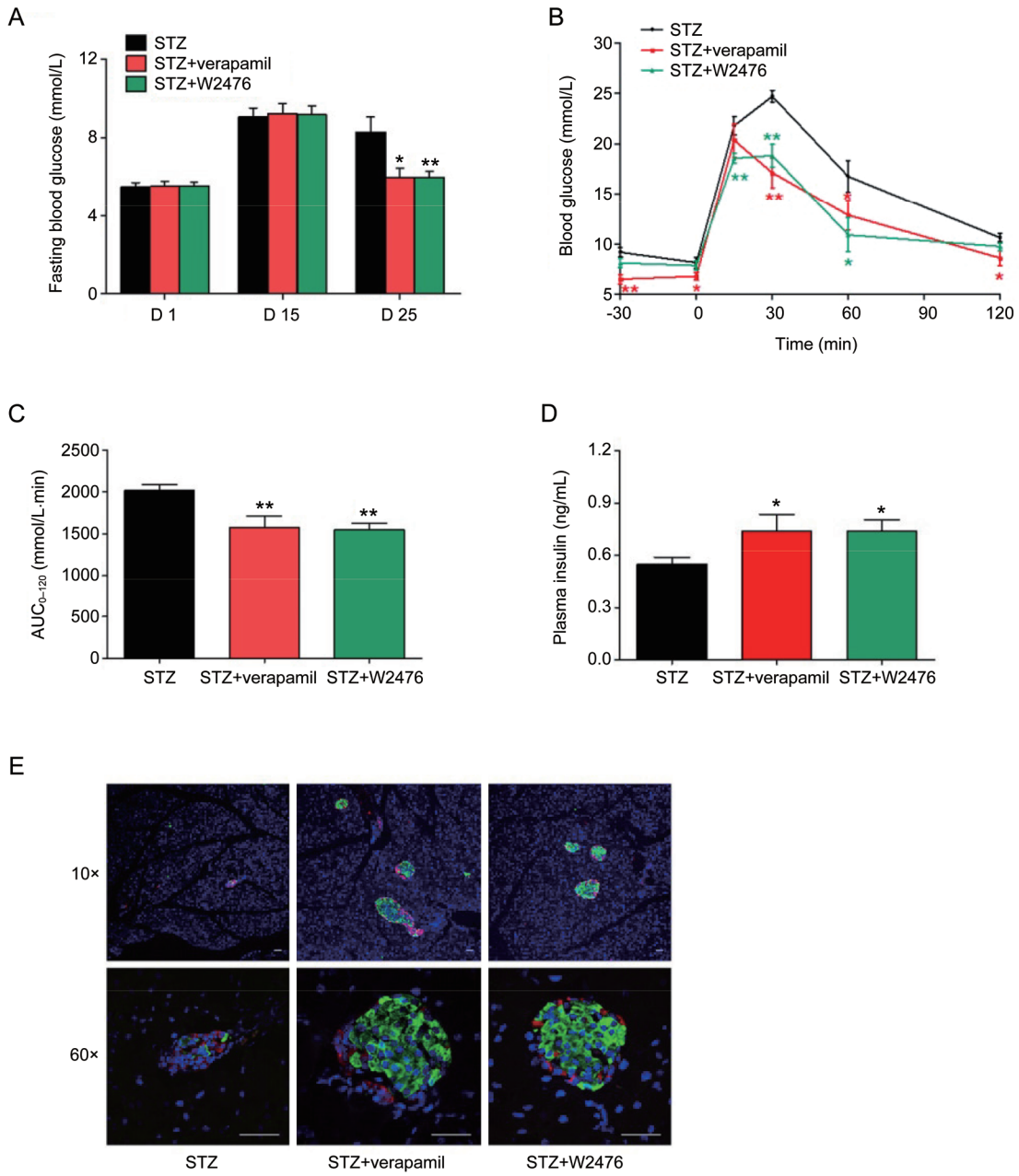


**Figure 5.** Therapeutic effect of W2476 on STZ-induced diabetic mice. Male C57BL/6 mice received daily intraperitoneal injection of STZ (40 mg·kg$^{-1}$·d$^{-1}$) for 5 d and rested for 10 d. On d 15, 6-h fasting blood glucose levels were measured, and those with glucose levels higher or equal to 8 mmol/L were selected to receive daily treatment of W2476 (200 mg/kg), verapamil (100 mg/kg) or vehicle (control). (A) Blood glucose levels measured on d 1, 15 and 25 ($n$=6 per group). Blood glucose levels (B) and $AUC_{0\text{-}120}$ (C) during OGTT on d 25. (D) Plasma insulin levels on d 25. (E) Immunofluorescence staining of pancreatic islets prepared from three groups following 10-d treatment. Red, glucagon; green, insulin; blue, nuclei/DAPI. Scale bar, 30 μm. Original magnification, 10× (upper panel) and 60× (lower panel). Data shown are mean±SEM. $^{*}P$<0.05, $^{**}P$<0.01 *vs* STZ group.

this cell-based assay system, exerted modulating action only in the high-glucose environment and had little impact when the glucose level was normal, as observed in CL108 cells. It is likely that W2476 may affect *trans*-acting factors bound to *cis*-acting elements located in the *txnip* gene[15]. The effect of W2476 was subsequently validated in INS-1E cells: it dose-dependently reduced both TXNIP mRNA and protein levels.

TXNIP is implicated in glucotoxicity and hence, β-cell apoptosis[17]. Consistent with previous findings that exenatide and verapamil could prevent β-cells from apoptosis by decreasing TXNIP expression[22, 31], we found that W2476 was also capable of protecting INS-1E cells from apoptosis induced by high glucose, probably through inhibition of the cleavage of caspase-3 and caspase-9. Impaired insulin transcription in diabetes appears to be involved in excessive β-cell expression of TXNIP: it is up-regulated in β-cells from diabetic subjects, and

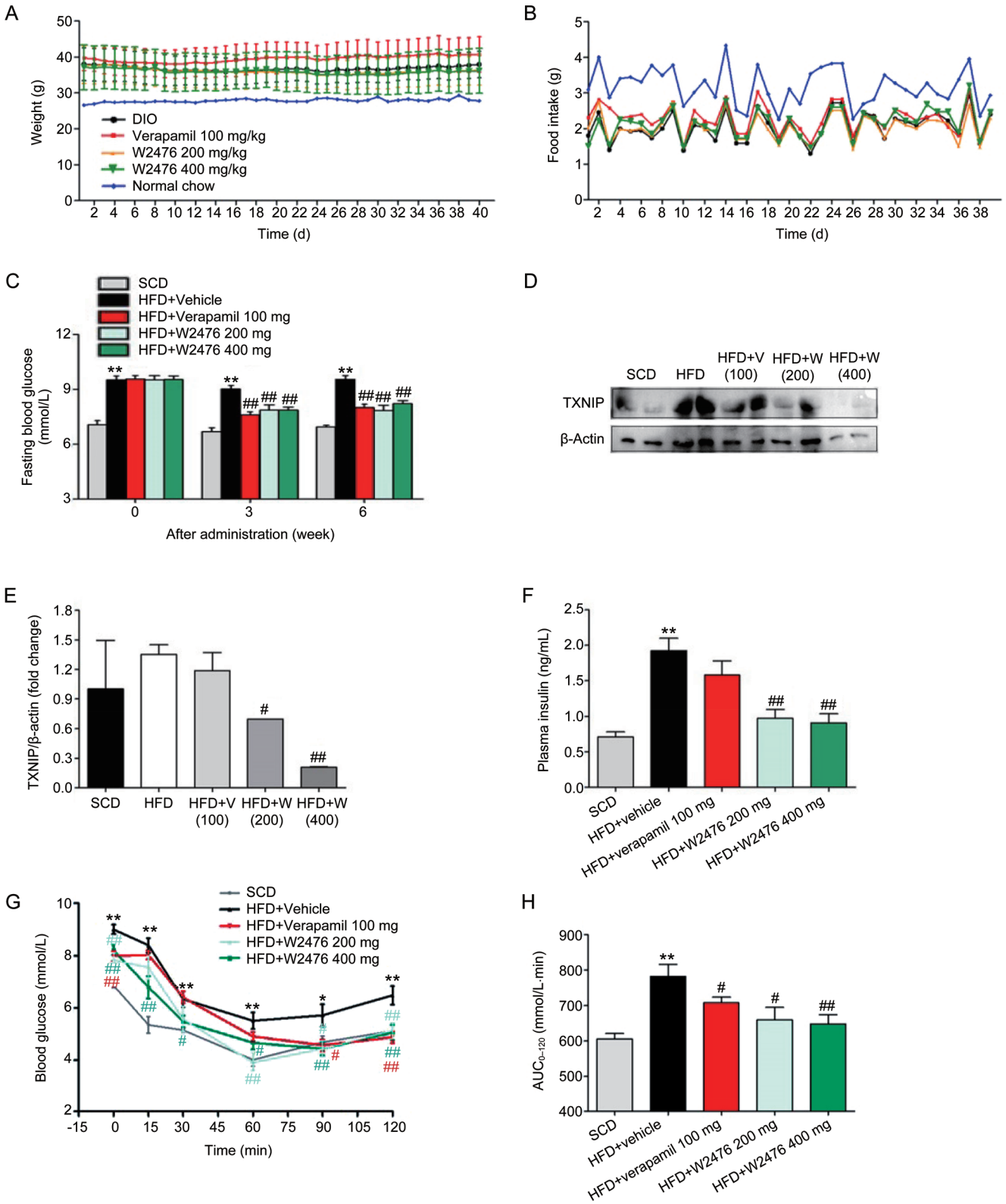


**Figure 6.** Protective effect of W2476 on DIO mice. Four-week-old male C57BL/6 mice were fed on SCD or HFD for 4 weeks. At approximately 8 weeks of age, they were treated with W2476 (200 or 400 mg·kg$^{-1}$·d$^{-1}$), verapamil (100 mg·kg$^{-1}$·d$^{-1}$) or vehicle for 6 weeks ($n$=11–12 per group). (A, B) Body weight on the last day of dosing and the average food intake during the 6-week treatment period. (C) The 6-h fasting blood glucose levels at weeks 0, 3 and 6. (D, E) Effects of W2476 and verapamil on pancreatic TXNIP protein levels in each group. At the end of treatment, plasma insulin levels were examined (F), and ITT was carried out to measure blood glucose response (G) and associated $AUC_{0-120}$ (H) in each group. Data shown are mean±SEM. $^{*}P$<0.05, $^{**}P$<0.01 *vs* SCD group. $^{\#}P$<0.05, $^{\#\#}P$<0.01 *vs* HFD group.

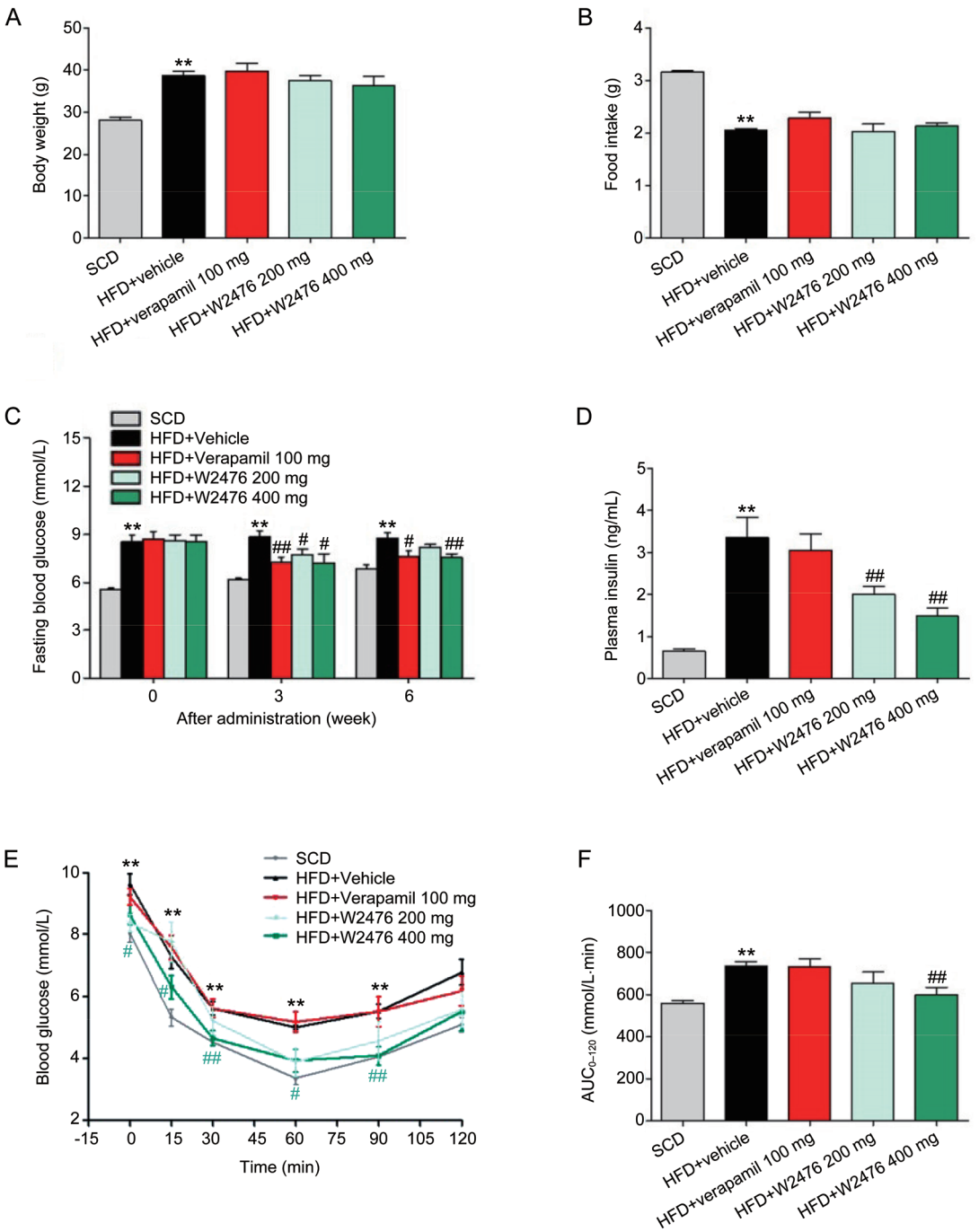


**Figure 7.** W2476 improves glucose homeostasis and insulin sensitivity in DIO mice. Male C57BL/6 mice fed on SCD or HFD for 12 weeks were chronically treated with W2476 (200 or 400 mg·kg$^{-1}$·d$^{-1}$), verapamil (100 mg·kg$^{-1}$·d$^{-1}$) or vehicle for 6 weeks ($n$=9 per group). (A) Body weight at the end of treatment. (B) Average daily food intake during the 6-week treatment period. (C) The 6-h fasting blood glucose levels at weeks 0, 3 and 6. (D) Plasma insulin levels following 6-week treatment. At the end of the experiment, ITT was carried out to measure blood glucose response (E) and associated $AUC_{0-120}$ (F) in each group. Data shown are mean±SEM. $^{*}P$<0.05, $^{**}P$<0.01 *vs* SCD group. $^{\#}P$<0.05, $^{\#\#}P$<0.01 *vs* HFD group.

its overexpression induces miR-204, leading to impaired MafA transcription and insulin production[18]. In this study, we have demonstrated that: (1) TXNIP was significantly elevated by high glucose; (2) this phenomenon was accompanied by down-regulation of MafA and insulin expression; (3) W2476 could reverse this course via modulation of TXNIP; and (4) most of these effects were confirmed in isolated rat islets of Langerhans. Failure of W2476 to rescue MafA mRNA levels might have resulted from the indifference of this transcription factor to 48 h stimulation by either 33.3 mmol/L or 5 mmol/L glucose in isolated rat islets (data not shown). These protective effects on β-cells exerted by W2476, including enhanced

β-cell mass by inhibiting apoptosis and improved function by increasing insulin production, appear to mimic those produced by TXNIP-deficient HcB-19 mice[16, 18].

TXNIP nonsense mutation (HcB-19) mice were found to exhibit lower blood glucose levels, increased β-cell mass and resistance to STZ-induced diabetes[46, 47]. bTKO mice also displayed defense against β-cell apoptosis induced by STZ injection[16]. In our *in vivo* experiments, a similar protective effect was observed in STZ-treated mice receiving W2476. Because verapamil was reported to inhibit β-cell TXNIP expression and prevent STZ-induced diabetes, it was applied as a positive control. Both W2476 and verapamil not only lowered blood glucose levels but also relieved diabetic symptoms and rescued β-cell loss in STZ-treated animals by lowering TXNIP. Our results are in line with previous reports that TXNIP deficient mice were resistant to STZ, and hence, development and progression of diabetes[39].

It has been demonstrated that disruption of TXNIP improved glucose homeostasis and ameliorated insulin sensitivity through activating insulin receptor substrate-1/Akt signaling[23]. Obesity is one of the most important factors in the development of insulin resistance. We employed a DIO model[41] to further elucidate the therapeutic property of W2476. Following induction with HFD, C57BL/6J mice exhibited significant increase in body weight and moderate hyperglycemia and hyperinsulinemia. After treatment with W2476 for 6 weeks, the fasting glucose level was markedly decreased without obvious changes in body weight and food intake. This observation is in agreement with the conclusion drawn from the investigations in HcB-19, TXNIP-deficient *ob/ob* and verapamil-treated BTBR *ob/ob* mice[16, 26, 31, 47].

DIO is characteristic of hyperinsulinemia and insulin resistance[41]. Following HFD induction, plasma insulin was significantly elevated in obese mice, which was corrected by 6-week treatment with W2476, but not verapamil. ITT results also support this phenomenon, *ie*, verapamil was less efficacious (prophylactic setting) or unable to (therapeutic setting) improve insulin sensitivity. Because verapamil, as a calcium channel blocker, interrupts intracellular calcium releases to affect insulin secretion and sensitivity[40], its behavior described above is expected.

The beneficial effects of W2476 on glucose homeostasis and insulin resistance were accompanied by improved plasma lipid profiles displaying reduced triacylglycerol and increased LDL-C/HDL-C ratio, whereas cholesterol and nonesterified fatty acid were not affected. This observation is not consistent with the finding showing high plasma free fatty acid levels in TXNIP-deficient mice[11]. The nature of such a difference remains to be explored. In spite of efforts made by multiple laboratories, little is known about the molecular mechanism(s) of TXNIP in regulating metabolism, although the modulating effects of W2476 were demonstrated in INS-1E cells, hepatocytes, myotubes and adipocytes (Figure S4). In this regard, W2476 may serve a valuable tool to elucidate the function of TXNIP.

In summary, a small molecule modulator of the TXNIP signaling pathway (W2476) was identified and preliminarily characterized *in vitro* and *in vivo*. W2476 improved β-cell dysfunction by protecting the cells against apoptosis and enhancing MafA and insulin expression. It exerted therapeutic properties in both STZ-induced diabetic and DIO mice. Our findings warrant further functional studies of ChREBP-regulated genes such as *txnip* to explore their potential application in treating T2DM.

## Acknowledgements

This work was partially supported by the National Health and Family Planning Commission (No 2012ZX09304-011, 2013ZX09401003-005, 2013ZX09507001 and 2013ZX09507-002), Shanghai Science and Technology Development Fund (No 15DZ2291600 and 14431901200), the Ministry of Science and Technology International Cooperation Program (No 2014DFG32200), Les Laboratories Servier (France) and the Thousand Talents Program in China. The authors declare no conflict of interest in the design, execution and publication of this article.

We are indebted to Xu SHEN, Cai-hong ZHOU, Ting XIAO, and Wen-juan HU for valuable discussions and technical assistance.

## Author contribution

Olivier NOSJEAN, Jean A BOUTIN, R PIERRE, and Ming-wei WANG conceived the idea. Ming-wei WANG, Olivier NOSJEAN, Ting LI, and Li ZHONG designed the study. Ting LI, Guang-yao LIN, Li ZHONG, Yan ZHOU, Jia WANG, Yue ZHU, Yang FENG, Xiao-qing CAI, and Qing LIU performed the experiments. Ting LI, Li ZHONG, De-hua YANG, and Ming-wei WANG analyzed the data and wrote the manuscript.

## Supplementary information

Supplementary information is available on the website of Acta Pharmacologica Sinica.

## References

1 Chen KS, Deluca HF. Isolation and characterization of a novel cDNA from HL-60 cells treated with 1,25-dihydroxyvitamin D-3. Biochim Biophys Acta 1994; 1219 : 26–32.

2 Nishiyama A, Matsui M, Iwata S, Hirota K, Masutani H, Nakamura H, *et al.* Identification of thioredoxin-binding protein-2/vitamin D(3) up-regulated protein 1 as a negative regulator of thioredoxin function and expression. J Biol Chem 1999; 274: 21645–50.

3 Yamanaka H, Maehira F, Oshiro M, Asato T, Yanagawa Y, Takei H, *et al.* A possible interaction of thioredoxin with VDUP1 in HeLa cells detected in a yeast two-hybrid system. Biochem Biophys Res Commun 2000; 271: 796–800.

4 Junn E, Han SH, Im JY, Yang Y, Cho EW, Um HD, *et al.* Vitamin D3 up-regulated protein 1 mediates oxidative stress via suppressing the thioredoxin function. J Immunol 2000; 164: 6287–95.

5 Nishiyama A, Masutani H, Nakamura H, Nishinaka Y, Yodoi J. Redox regulation by thioredoxin and thioredoxin-binding proteins. IUBMB Life 2001; 52: 29–33.

6 Patwari P, Higgins LJ, Chutkow WA, Yoshioka J, Lee RT. The interaction of thioredoxin with txnip — evidence for formation of a mixed disulfide

by disulfide exchange. J Biol Chem 2006; 281: 21884–91.
7 Fould B, Lamamy V, Guenin SP, Ouvry C, Coge F, Boutin JA, *et al*. Mutagenic analysis in a pure molecular system shows that thioredoxin-interacting protein residue Cys247 is necessary and sufficient for a mixed disulfide formation with thioredoxin. Protein Sci 2012; 21: 1323–33.
8 Zhou R, Tardivel A, Thorens B, Choi I, Tschopp J. Thioredoxin-interacting protein links oxidative stress to inflammasome activation. Nat Immunol 2010; 11: 136–40.
9 Nishinaka Y, Nishiyama A, Masutani H, Oka S, Ahsan KM, Nakayama Y, *et al.* Loss of thioredoxin-binding protein-2/vitamin $D_3$ up-regulated protein 1 in human T-cell leukemia virus type I-dependent T-cell transformation: implications for adult T-cell leukemia leukemogenesis. Cancer Res 2004; 64: 1287–92.
10 Oka S, Yoshihara E, Bizen-Abe A, Liu W, Watanabe M, Yodoi J, *et al*. Thioredoxin binding protein-2/thioredoxin-interacting protein is a critical regulator of insulin secretion and peroxisome proliferator-activated receptor function. Endocrinology 2009; 150: 1225–34.
11 Oka S, Liu W, Masutani H, Hirata H, Shinkai Y, Yamada S, *et al.* Impaired fatty acid utilization in thioredoxin binding protein-2 (TBP-2)-deficient mice: a unique animal model of reye syndrome. FASEB J 2006; 20: 121–3.
12 Schulze PC, Yoshioka J, Takahashi T, He ZH, King GL, Lee RT. Hyperglycemia promotes oxidative stress through inhibition of thioredoxin function by thioredoxin-interacting protein. J Biol Chem 2004; 279: 30369–74.
13 Minn AH, Hafele C, Shalev A. Thioredoxin-interacting protein is stimulated by glucose through a carbohydrate response element and induces β-cell apoptosis. Endocrinology 2005; 146: 2397–405.
14 Stoltzman CA, Peterson CW, Breen KT, Muoio DM, Billin AN, Ayer DE. Glucose sensing by MondoA: Mlx complexes: A role for hexokinases and direct regulation of thioredoxin-interacting protein expression. Proc Natl Acad Sci U S A 2008; 105: 6912–7.
15 Cha-Molstad H, Saxena G, Chen JQ, Shalev A. Glucose-stimulated expression of TXNIP is mediated by carbohydrate response element-binding protein, p300, and histone H4 acetylation in pancreatic β-cells. J Biol Chem 2009; 284: 16898–905.
16 Chen JQ, Hui ST, Couto FM, Mungrue IN, Davis DB, Attie AD, *et al.* Thioredoxin-interacting protein deficiency induces Akt/Bcl-xL signaling and pancreatic β-cell mass and protects against diabetes. FASEB J 2008; 22: 3581–94.
17 Chen J, Saxena G, Mungrue IN, Lusis AJ, Shalev A. Thioredoxin-interacting protein — a critical link between glucose toxicity and β-cell apoptosis. Diabetes 2008; 57: 938–44.
18 Xu GL, Chen JQ, Jing G, Shalev A. Thioredoxin-interacting protein regulates insulin transcription through microRNA-204. Nat Med 2013; 19: 1141–6.
19 Fukushima T, Sasaki H. Metabolic disorder (diabetes mellitus, hypoglycemia, hyperglycemia, insulin resistance). Nihon Rinsho 2004; 62 Suppl: 379–83.
20 Saxena G, Chen J, Shalev A. Intracellular shuttling and mitochondrial function of thioredoxin-interacting protein. J Biol Chem 2010; 285: 3997–4005.
21 Robertson RP, Harmon J, Tran PO, Tanaka Y, Takahashi H. Glucose toxicity in β-cells: type 2 diabetes, good radicals gone bad, and the glutathione connection. Diabetes 2003; 52: 581–7.
22 Chen J, Couto FM, Minn AH, Shalev A. Exenatide inhibits β-cell apoptosis by decreasing thioredoxin-interacting protein. Biochem Biophys Res Commun 2006; 346: 1067–74.
23 Yoshihara E, Fujimoto S, Inagaki N, Okawa K, Masaki S, Yodoi J, *et al.* Disruption of TBP-2 ameliorates insulin sensitivity and secretion without affecting obesity. Nat Commun 2010; 1: 127.
24 Parikh H, Carlsson E, Chutkow WA, Johansson L, Saxena R, Krook A, *et al.* Identification of TXNIP as a marker and regulator of glucose homeostasis in humans. Diabetologia 2006; 49: 21.
25 Wu N, Zheng B, Shaywitz A, Dagon Y, Tower C, Bellinger G, *et al.* AMPK-dependent degradation of TXNIP upon energy stress leads to enhanced glucose uptake via GLUT1. Mol Cell 2013; 49: 1167–75.
26 Hui TY, Sheth SS, Diffley JM, Potter DW, Lusis AJ, Attie AD, *et al.* Mice lacking thioredoxin-interacting protein provide evidence linking cellular redox state to appropriate response to nutritional signals. J Biol Chem 2004; 279: 24387–93.
27 Chutkow WA, Patwari P, Yoshioka J, Lee RT. Thioredoxin-interacting protein (TXNIP) is a critical regulator of hepatic glucose production. J Biol Chem 2008; 283: 2397–406.
28 Kim JB, Spiegelman BM. ADD1/SREBP1 promotes adipocyte differentiation and gene expression linked to fatty acid metabolism. Genes Dev 1996; 10: 1096–107.
29 Luo X, Li T, Zhu Y, Dai Y, Zhao J, Guo ZY, *et al.* The insulinotrophic effect of insulin-like peptide 5 *in vitro* and *in vivo*. Biochem J 2015; 466: 467–73.
30 Seglen PO. Preparation of isolated rat liver cells. Methods Cell Biol 1976; 13: 29–83.
31 Xu G, Chen J, Jing G, Shalev A. Preventing β-cell loss and diabetes with calcium channel blockers. Diabetes 2012; 61: 848–56.
32 He M, Su H, Gao W, Johansson SM, Liu Q, Wu X, *et al.* Reversal of obesity and insulin resistance by a non-peptidic glucagon-like peptide-1 receptor agonist in diet-induced obese mice. PLoS One 2010; 5: e14205.
33 Zhang JH, Chung TDY, Oldenburg KR. A simple statistical parameter for use in evaluation and validation of high throughput screening assays. J Biomol Screen 1999; 4: 67–73.
34 Cadenas C, Franckenstein D, Schmidt M, Gehrmann M, Hermes M, Geppert B, *et al.* Role of thioredoxin reductase 1 and thioredoxin interacting protein in prognosis of breast cancer. Breast Cancer Res 2010; 12: R44.
35 Dutta KK, Nishinaka Y, Masutani H, Akatsuka S, Aung TT, Shirase T, *et al.* Two distinct mechanisms for loss of thioredoxin-binding protein-2 in oxidative stress-induced renal carcinogenesis. Lab Invest 2005; 85: 798–807.
36 Kwon HJ, Won YS, Suh HW, Jeon JH, Shao Y, Yoon SR, *et al.* Vitamin D-3 upregulated protein 1 suppresses TNFα-induced NF-κB activation in hepatocarcinogenesis. J Immunol 2010; 185: 3980–9.
37 Lee JH, Jeong EG, Choi MC, Kim SH, Park JH, Song SH, *et al.* Inhibition of histone deacetylase 10 induces thioredoxin-interacting protein and causes accumulation of reactive oxygen species in SNU-620 human gastric cancer cells. Mol Cell 2010; 30: 107–12.
38 Takahashi Y, Nagata T, Ishii Y, Ikarashi M, Ishikawa K, Asai S. Up-regulation of vitamin $D_3$ up-regulated protein 1 gene in response to 5-fluorouracil in colon carcinoma SW620. Oncol Rep 2002; 9: 75–9.
39 Masson E, Koren S, Goldberg H, Kwan E, Gaisano H, Fantus IG. Hcb-19/TxNIP$^{(-/-)}$ mice are resistant to streptozotocin (STZ)-induced diabetes. Diabetes 2008; 57 Suppl 1: A65.
40 Chen J, Cha-Molstad H, Szabo A, Shalev A. Diabetes induces and calcium channel blockers prevent cardiac expression of proapoptotic thioredoxin-interacting protein. Am J Physiol Endocrinol Metab 2009; 296: E1133–9.
41 Winzell MS, Ahren B. The high-fat diet-fed mouse: a model for studying mechanisms and treatment of impaired glucose tolerance and type 2 diabetes. Diabetes 2004; 53 Suppl 3: S215–9.
42 Katsumi I, Yukio H. ChREBP A glucose-actived transcription factor involved in the development of metabolic syndrome. Endocr J 2008;

55: 617–24.

43 Poupeau A, Postic C. Cross-regulation of hepatic glucose metabolism via ChREBP and nuclear receptors. Biochim Biophys Acta 2011; 1812: 995–1006.

44 Shalev A, Pise-Masison CA, Radonovich M, Hoffmann SC, Hirshberg B, Brady JN, *et al.* Oligonucleotide microarray analysis of intact human pancreatic islets: Identification of glucose-responsive genes and a highly regulated TGF-β signaling pathway. Endocrinology 2002; 143: 3695–8.

45 Parikh H, Carlsson E, Chutkow WA, Johansson LE, Storgaard H, Poulsen P, *et al.* TXNIP regulates peripheral glucose metabolism in humans. PLoS Med 2007; 4: 868–79.

46 Masson E, Koren S, Razik F, Goldberg H, Kwan EP, Sheu L, *et al.* High β-cell mass prevents streptozotocin-induced diabetes in thioredoxin-interacting protein-deficient mice. Am J Physiol Endocrinol Metab 2009; 296: E1251–61.

47 Sheth SS, Castellani LW, Chari S, Wagg C, Thipphavong CK, Bodnar JS, *et al.* Thioredoxin-interacting protein deficiency disrupts the fasting-feeding metabolic transition. J Lipid Res 2005; 46: 123–34.